



Structure–activity relationships of a peptide inhibitor of the human FcRn:human IgG interaction

Adam R. Mezo^{a,*}, Kevin A. McDonnell^a, Alfredo Castro^b, Cara Fraley^a

^a Syntonix Pharmaceuticals, Inc., 9 Fourth Avenue, Waltham, MA 02451, USA

^b Infinity Pharmaceuticals, Inc., 780 Memorial Drive, Cambridge, MA 02139, USA

ARTICLE INFO

Article history:

Received 10 January 2008

Revised 1 May 2008

Accepted 2 May 2008

Available online 6 May 2008

Keywords:

Neonatal Fc receptor

FcRn

Autoimmune disease

Peptide antagonist

Peptidomimetic

Inhibition

ABSTRACT

A family of five peptides was previously discovered by phage display techniques that binds to the human neonatal Fc receptor (FcRn) and inhibits the human IgG:human FcRn protein–protein interaction [*Proc. Nat. Acad. Sci. U.S.A.* **2008**, *105*, 2337–2342]. The consensus peptide motif consists of the sequence **GHFGGXY** where **X** is preferably a hydrophobic amino acid, and also includes a disulfide bridge enclosing 11-amino acids in varying positions about the consensus sequence. We describe herein the structure–activity relationships of one of the five peptides in binding to FcRn using surface plasmon resonance and IgG:FcRn competition ELISA assays. Modifications of the peptide length, cyclization, and the incorporation of amino acid substitutions and dipeptide mimetics were studied. The most potent analogs exhibited a 50- to 100-fold improvement of in vitro activity over that of the phage-identified peptide sequence.

© 2008 Elsevier Ltd. All rights reserved.

1. Introduction

The neonatal Fc receptor, FcRn, is the key regulatory protein for IgG homeostasis in animals.^{1,2} Extensive studies over many years have confirmed that FcRn is a saturable salvage receptor for IgG in circulation and provides these large proteins with their unusually long circulating half-lives. For example, it has been reported that the serum half-life of IgG in normal mice is 9 days versus only 1.4 days in FcRn-deficient mice.³ FcRn is broadly expressed in endothelial cells⁴ as well as in bone marrow-derived phagocytic cells.⁵ It is thought that IgG undergoes fluid phase pinocytosis to gain entry into cells and then bypasses the lysosomal degradation pathway by binding to FcRn in the acidic (pH 6) environment of the endosome.⁶ IgG is then shuttled back to the cell surface and released by exocytosis⁷ into circulation since IgG has minimal affinity for FcRn at the extracellular pH of 7.4.

FcRn is thus a potential therapeutic target for treating autoimmune diseases where the reduction of pathogenic IgGs could have therapeutic benefits. Indeed, research using FcRn-deficient mice has demonstrated therapeutic benefits in a model for rheumatoid arthritis⁸ and various skin blistering diseases.⁹ Furthermore, recent reports have demonstrated that targeting FcRn with an appropriate antagonist in vivo can be relevant in treating autoimmune disease states. For example, a monoclonal antibody targeting FcRn reduced symptoms of experimental autoimmune myasthenia gravis (EAMG)

in rats.¹⁰ In addition, a human IgG antibody genetically engineered for higher affinity binding to human FcRn (hFcRn) was found to ameliorate experimental arthritis in FcRn-transgenic mice.¹¹

We previously discovered a family of five novel peptides that is capable of binding to hFcRn and blocking IgG binding.¹² These five peptides, SYN722–SYN726 (Table 1), formed the basis of a consensus FcRn-binding motif: **GHFGGXY**, where **X** is preferably a hydrophobic amino acid. The motif is enclosed by a cysteine disulfide loop where the loop contains 11 amino acids including the cysteines. Chemical optimization of SYN722 and its homodimerization to form SYN1436 resulted in greatly enhanced in vitro activity and resulted in dramatic in vivo effects. SYN1436 accelerated the catabolism of IgG in both transgenic mice possessing human FcRn and in cynomolgus monkeys, while its constituent monomeric peptide SYN1327 was inactive in the same transgenic mouse experiment.¹² Herein we describe the structure–activity relationships of the core peptide sequence of SYN722 and its chemical optimization into the optimized monomeric peptide SYN1327. Structure–activity relationships relating to the dimerization of the peptide monomers will be described elsewhere.

2. Results

2.1. Consensus peptide motif

The peptide hits derived from the phage display screen¹² and the corresponding consensus motif are shown in Table 1. The consensus motif is enclosed by an 11-amino acid disulfide loop with

* Corresponding author. Tel.: +1 781 547 5228; fax: +1 781 547 6008.

E-mail address: amezo@syntn.com (A.R. Mezo).

Table 1
Phage hit peptide sequences

Peptide No.	Sequence ^a	IC ₅₀ ^b (μM)	K _d ^c (pH 6) (μM)	K _d ^c (pH 7.4) (μM)
SYN722	QRFC <u>CTGHFGGLY</u> PCNGP	36	5.7	45
SYN723	GGGCVT <u>GHFGGIY</u> CNYQ	33	5.2	35
SYN724	KII <u>CS</u> PGHFGGM <u>YC</u> QCGK	64	22	78
SYN725	PSY <u>CIEGHIDGIY</u> CFNA	49	8.8	76
SYN726	NSFCRGRPGHFGG <u>CY</u> LF	33	9.4	93
Consensus	GHFGGXY			

^a Peptides were synthesized with flanking AG residues on the N-terminus and GTGGGK residues on the C-terminus to reflect the non-variable flanking residues found in the phage library during the screen. Disulfide bonds link the underlined cysteines.

^b IC₅₀ values were determined using the IgG competition ELISA assay as described in the text.

^c K_d values were determined using the SPR assay as described in the text.

cysteines at *varying* positions relative to the consensus motif. For example, in SYN722, the C-terminal cysteine resides two amino acids from the end of the consensus motif, while in SYN723–SYN725, the C-terminal cysteine is directly adjacent to the C-terminal residue of the motif. Furthermore, in SYN726, the C-terminal cysteine resides *within* the consensus motif at position **X**. SYN722 was selected for more detailed studies and optimization since it was one of the highest affinity of the five peptide sequences and was the most prominent sequence selected in the phage screening process.

2.2. In vitro assays

Two different assays were used to study the in vitro activity of the peptides, as described previously.¹² The first was a surface plasmon resonance (SPR) assay where soluble human FcRn was immobilized on the chip surface while soluble peptides are allowed to flow over the chip. From these SPR experiments, dissociation constants (K_d) for the peptide:FcRn interaction were obtained. The second assay was a competition assay between human IgG at a constant concentration (3 nM) and peptide at varying concentrations for binding to immobilized soluble human FcRn on 96-well plates. The concentration of peptide that was needed to inhibit 50% of the IgG:FcRn interaction was determined and reported as its IC₅₀ value. Both the K_d and IC₅₀ are referred to in the Tables.

2.3. Truncations of SYN722

SYN722 was truncated at both the N- and C-termini to determine the shortest sequence possessing full binding and inhibitory characteristics (Table 2, Fig. 1). Truncations of residues from the C-terminus up to the cysteine residue did not affect activity. In contrast, the N-terminal residues appeared to be required for full activity. Also note peptide **4** which contains the core motif without the benefit of the cysteine disulfide; this peptide is inactive up to 250 μM which demonstrates that cyclization greatly enhances activity.

2.4. Alanine scan of SYN746

Several residues in the sequence of SYN746 were replaced with alanine to gauge their impact on peptide activity (Table 3). As expected, when each amino acid in the consensus motif (apart from X) was changed to alanine, a significant loss in activity was observed. Amino acid position X in the motif (in this case, leucine) was still moderately active when replaced with alanine which suggests only a bias towards hydrophobic or bulky amino acids at this position.

Table 2
Truncations of SYN722

Peptide No.	Sequence	IC ₅₀ (μM)	K _d (pH 6) (μM)
SYN722	AGQRFCCTGHFGGLYPCNGPCTGGGK	36	5.7
SYN746	QRFCCTGHFGGLYPCNGP	40 ± 15 (n = 4)	5.1
1	CTGHFGGLYPCNGP	239	34
2	QRFCCTGHFGGLYPC	27	4.2
3	CTGHFGGLYPC	110	20
4	TGHFGGLYP	>250	>250
5	RFCTGHFGGLYPCNGP	24	2.9
6	FGTGHFGGLYPCNGP	67	11
7	QRFCCTGHFGGLYPCNG	34	4.6
8	QRFCCTGHFGGLYPCN	31	6.1
9	RFCTGHFGGLYPC	87	10

2.5. Cysteine analogs

The effect of incorporating cysteine analogs was studied by replacing the two cysteines systematically with homocysteine, D-cysteine and penicillamine (Table 4). The introduction of homocysteine had no effect on the activity of the peptide while the introduction of D-cysteine greatly reduced binding. In contrast, introduction of L-penicillamine (Pen) into the N-terminal cysteine position *enhanced* activity by approximately 10- to 20-fold in these assays (peptide **27**). Incorporation of Pen into the C-terminal cysteine position had only a limited effect (peptide **28**), while the incorporation of two Pen residues resulted in no additional enhancement of binding or blocking activity over that of peptide **27**.

2.6. Truncations of SYN775

With the discovery of the enhancing effect of penicillamine, truncations of peptide **27** were investigated (Table 5). It was found that both Gln1 and Arg2 could be removed with minimal loss in activity. Note that the inclusion of the C-terminal 'NGP' is inconsequential to the activity of the peptide (Table 2).

2.7. N-Methyl scan

The incorporation of N-methyl residues can enhance the stability of peptides to enzymatic degradation and thus render peptides more active in vivo.¹³ We substituted N-methyl residues for their natural counterparts and studied their effects on in vitro activity (Table 6). The addition of a N-methyl group to amino acids Gly6, His7, Phe8, and Tyr12 (peptides **35,36,37,41**) reduced the peptide activity >100-fold. The addition of sarcosine for Gly9 (peptide **38**) reduced peptide activity approximately 10-fold. It is possible that the amide protons of these amino acids are involved in critical hydrogen bonding interactions. Interestingly, the incorporation of sarcosine for Gly10 enhanced binding and blocking activity approximately 2-fold (peptide **39**). Incorporation of N-methyl leucine (NMeLeu) at position 11 enhanced the binding activity approximately 3-fold and marginally enhanced its blocking activity (peptide **40**). Combining these two favorable substitutions (peptide **44**, SYN1327) resulted in a 4- to 5-fold enhancement in binding activity over that of peptide **27**.

2.8. Analogs of glycine in SYN746

The presence of three glycine residues in the consensus motif may be due to the need for amino acid torsional angles not accessible with L-amino acids and therefore unavailable in the phage display screen. To study this possibility, peptides incorporating the substitution of D-alanine for glycine were synthesized

Ac-Gln1-Arg2-Phe3-Cys4-Thr5-**Gly6-His7-Phe8-Gly9-Gly10-Leu11-Tyr12**-Pro13-Cys14-Asn15-Gly16-Pro17-CONH₂

Figure 1. Numbering convention for SYN746. Residues underlined and in bold represent the consensus motif.

Table 3

Alanine scan of SYN746

Peptide No.	Sequence	IC ₅₀ (μM)	K _d (pH 6) (μM)
SYN746	QRFCTGHFGGLYPCNGP	40 ± 15 (n = 4)	5.1
10	Q A FCTGHFGGLYPCNGP	23	7.7
11	Q R A C TGHFGGLYPCNGP	95	28
12	Q R F C A G HFGGLYPCNGP	30	4.9
13	Q R F C T A HFGGLYPCNGP	>125	>250
14	Q R F C T G A F GGLYPCNGP	>125	>250
15	Q R F C T G H A GGLYPCNGP	>125	>250
16	Q R F C T G H F A G LYPCNGP	>125	230
17	Q R F C T G H F C A LYPCNGP	>125	120
18	Q R F C T G H F G G A Y PCNGP	107	26
19	Q R F C T G H F G G L A PCNGP	>125	>250
20	Q R F C T G H F G G L A CNGP	96	14
21	Q R F C T G H F G G L C A G P	30	8

Table 4

Cysteine derivatives of SYN746

Peptide No.	Sequence ^a	IC ₅₀ (μM)	K _d (pH 6) (μM)
SYN746	QRF-C-TGHFGGLYP-C-NGP	40 ± 15 (n = 4)	5.1
22	QRFCTGHFGGLYP- hC -NGP	21	3.9
23	QRF- hC -TGHFGGLYP- hC -NGP	20	3.8
24	QRF- c -TGHFGGLYP-C-NGP	>125	150
25	QRF-C-TGHFGGLYP- c -NGP	125	31
26	QRF- c -TGHFGGLYP- c -NGP	>500	200
27	QRF-Pen-TGHFGGLYP-C-NGP	2	0.25
28	QRF-C-TGHFGGLYP-Pen-NGP	18	2.7
29	QRF-Pen-TGHFGGLYP-Pen-NGP	2	0.37
30	QRF-Pen-TGHFGGLYP- hC -NGP	2	0.31
31	QRF- hC -TGHFGGLYP-Pen-NGP	16	2.1

^a 'Pen', L-penicillamine; 'hC' = L-homocysteine; 'c' = D-cysteine.

Table 5

Truncations of peptide 27 derivatives

Peptide No.	Sequence	IC ₅₀ (μM)	K _d (pH 6) (μM)
27	QRF-Pen-TGHFGGLYPCNGP	2	0.25
32	F-Pen-TGHFGGLYPC	1.7	0.31
33	RF-Pen-TGHFGGLYPC	2.0	0.17

Table 6

N-Methyl derivatives of SYN746 and peptide 27

Peptide No.	Sequence ^a	IC ₅₀ (μM)	K _d (pH 6) (μM)
SYN746	QRFCTGHFGGLYPCNGP	40 ± 15 (n = 4)	5.1
34	QRF-C-NMeAla-GHFGGLYPCNGP	169	18
27	QRF-Pen-TGHFGGLYP-C-NGP	2	0.25
35	QRF-Pen-T-Sar-HFGGLYP-C-NGP	>125	88
36	RF-Pen-TG-NMeHis-FGLYPC	>250	nd
37	QRF-Pen-TGH-NMePhe-GGLYPCNGP	>125	>250
38	QRF-Pen-TGHF-Sar-GLYPCNGP	27	2
39	QRF-Pen-TGHFG-Sar-LYPCNGP	0.9	0.11
40	QRF-Pen-TGHFGG-NMeLeu-YPNGP	1.6	0.086
41	QRF-Pen-TGHFGGL-NMeTyr-PCNGP	>125	92
42	RF-Pen-TGHFGG-NMeLeu-YP	2.1	0.059
43	RF-Pen-TGHFG-Sar-YP	1.0	0.058
44	QRF-Pen-TGHFG-Sar-NMeLeu-YPNGP	0.42	0.046
SYN1327	RF-Pen-TGHFG-Sar-NMeLeu-YP	0.49	0.031

^a 'Sar', sarcosine; 'NMe' prefix denotes N-methyl amino acid.

(Table 7). Substitution of D-alanine for Gly6 (peptide 45) resulted in a >200-fold weaker affinity which confirms the strict requirement for glycine in this position since L-alanine was also greatly inactivating in this position (Table 3). Further incorporation of a methylene group into the peptide backbone by substitution of Gly6 with β-alanine also rendered the peptide inactive (peptide 49). These data suggest that Gly6 is ideally suited for this position and that there may be steric limitations to incorporating additional functionality. However, this was not the case for Gly9 and Gly10. The substitution of D-alanine for glycine in these positions resulted in only a two-fold loss in activity. This is in contrast to the >10-fold loss in activity when substituted with L-alanine (Table 3). This suggests that the amino acid torsional angles of these two residues more closely resemble D-amino acids and therefore may be a useful starting point for the synthesis of peptidomimetics in this portion of the peptide sequence.

To further study the possibility of increasing the potency of peptide 27 using D-amino acid substitutions in the Gly9-Gly10 position, various D-amino acids were placed in the Gly9 and/or Gly10 positions (Table 8). These peptides included the known β-hairpin nucleators D-Pro-L-Pro¹⁴ as well as the type II' turn nucleators D-Pro-Gly and D-Phe-L-Pro.^{15,16} Of all the peptides, only the dipeptide Gly-D-Pro (peptide 50) was equipotent to the Gly9-Gly10 dipeptide. None of the substitutions resulted in enhanced in vitro activity.

2.9. D-Amino acid scan of SYN775

The effect of substituting D-amino acids for L-amino acids in the rest of the peptide was studied in the context of peptide 27 (Table 9). Many of the positions were incompatible with D-amino acids, which suggests great specificity for the consensus motif. The Gly9 and Gly10 positions are shown replaced with D-alanine and these analogs were only modestly less active (vide supra).

2.10. Analogs of Phe8

A number of aromatic analogs of Phe8 were synthesized and studied, to probe the hydrophobic surface surrounding the phenyl ring (Table 10). Although some methyl-Phe derivatives appear to be demonstrate slightly greater activity (peptides 93 and 95), no significant increase in activity was observed. The introduction of potential hydrogen bonding donors (e.g., 4-acetamido-Phe: peptide 98) and acceptors (e.g., pyridylalanines: peptides 88–90) around the ring also resulted in decreased activity. Overall, the binding of peptide 27 to shFcRn is highly specific for a single hydrophobic phenyl ring.

Table 7

Analogs of glycine in SYN746

Peptide No.	Sequence ^a	IC ₅₀ (μM)	K _d (pH 6) (μM)
SYN746	QRFCTGHFGGLYPCNGP	40 ± 15 (n = 4)	5.1
45	QRFCT- a -HFGGLYPCNGP	>125	>250
46	QRFCTGHF- a -GLYPCNGP	48	10
47	QRFCTGHFG- a -LYPCNGP	57	12
48	QRFCTGHF- a -a-LYPCNGP	69	22
49	QRFCT-βAla-HFGGLYPCNGP	>125	>250

^a 'a', D-alanine; 'βAla' = β-alanine.

Table 8Analogues of peptide **27** at Gly9-Gly10-Leu11

Peptide No.	Sequence ^a	IC ₅₀ (μM)	K _d (pH 6) (μM)
27	QRF-Pen-TGHF-GG-LYP-C-NGP	2	0.25
50	QRF-Pen-TGHF-G-p-LYPCNGP	1.4	0.23
51	QRF-Pen-TGHF-G-r-LYPCNGP	8.1	0.83
52	QRF-Pen-TGHF-G-h-LYPCNGP	12	2
53	QRF-Pen-TGHF-G-i-LYPCNGP	18	2.2
54	QRF-Pen-TGHF-G-f-LYPCNGP	13	1.7
55	QRF-Pen-TGHF-G-y-LYPCNGP	13	1.5
56	QRF-Pen-TGHF-G-Aib-LYPCNGP	2.4	0.48
57	QRF-Pen-TGHF-d-G-LYPCNGP	3.1	0.58
58	QRF-Pen-TGHF-p-G-LYPCNGP	5	0.79
59	QRF-Pen-TGHF-r-G-LYPCNGP	4.1	0.31
60	QRF-Pen-TGHF-h-G-LYPCNGP	3.6	0.41
61	QRF-Pen-TGHF-l-G-LYPCNGP	9.4	2.6
62	QRF-Pen-TGHF-f-G-LYPCNGP	2.8	0.51
63	QRF-Pen-TGHF-y-G-LYPCNGP	3.2	0.32
64	QRF-Pen-TGHF-Aib-G-LYPCNGP	17	5.2
65	QRF-Pen-TGHF-G-a-LYPCNGP	2	0.48
66	QRF-Pen-TGHF-a-G-LYPCNGP	4.5	0.49
67	QRF-Pen-TGHF-a-a-LYPCNGP	4.5	0.45
68	QRF-Pen-TGHF-a-p-LYPCNGP	3.7	0.43
69	QRF-Pen-TGHF-f-p-LYPCNGP	5.9	0.72
70	QRF-Pen-TGHF-f-a-LYPCNGP	4.3	0.41
71	QRF-Pen-TGHF-p-p-LYPCNGP	21	3.3
72	QRF-Pen-TGHF-f-G-NMeLeu- YPCNGP	1.3	0.24
73	QRF-Pen-TGHF-a-G-NMeLeu- YPCNGP	3.2	0.23 ± 0.03 (n = 4)
74	QRF-Pen-TGHF-f-G-P-YPCNGP	39	18.3
75	QRF-Pen-TGHF-p-P-LYPCNGP	>250	>100
76	QRF-Pen-TGHF-f-P-LYPCNGP	22	3.8
77	QRF-Pen-TGHF-a-Sar-LYPCNGP	1.7	0.19

^a 'Aib', aminoisobutyric acid.**Table 9**D-Amino acid scan of peptide **27**

Peptide No.	Sequence	IC ₅₀ (μM)	K _d (pH 6) (μM)
27	QRF-Pen-TGHFGGLYP-C-NGP	2	0.25
78	Q-I-F-Pen-TGHFGGLYP-C-NGP	1.7	0.28
79	Q-R-F-Pen-TGHFGGLYP-C-NGP	11.4	1.8
80	QRF-Pen-I-GHFGGLYP-C-NGP	>125	>250
81	QRF-Pen-TGH-f-GGLYP-C-NGP	>125	>250
66	QRF-Pen-TGHF-a-GLYP-C-NGP	4.5	0.49
65	QRF-Pen-TGHFG-a-LYP-C-NGP	2	0.48
82	QRF-Pen-TGHFGG-l-YP-C-NGP	>125	>250
83	QRF-Pen-TGHFGGL-y-P-C-NGP	>125	>250
84	QRF-Pen-TGHFGGLY-p-C-NGP	>125	>250

2.11. Analogs of Tyr12

The specificity for tyrosine at position 12 was studied by incorporating similar analogs. Of the analogs assayed (Table 11), the peptide motif was very specific for the tyrosine side-chain in this position. For example, the 4-amino-Phe analog peptide 110, which might be expected to exhibit similar hydrogen bonding characteristics, was >50-fold less active. In addition, capping of the phenolic side-chain with a methyl group (peptide 111) or removal of the hydroxyl group (peptide 109) also resulted in a dramatic loss in activity. These data suggest a critical role for the phenolic moiety as both a potential hydrogen bond donor and acceptor. Interestingly, the 4-fluoro-phenylalanine derivative (peptide 117) lost only ~10-fold activity indicating that the fluorine atom may be capable of partially mediating the same interaction as the phenolic moiety.

2.12. Analogs of His7

Histidine was also one of the critical residues found in the alanine scan. The presence of histidine suggests a possible pH-depen-

dence of binding to FcRn due to the pK_a of histidine which is approximately 6.5. Indeed, for all of the peptide derivatives described thus far, the K_d for binding FcRn is typically about 5-fold tighter at pH 6 than at pH 7.4. This suggests that the mechanism of peptide binding to shFcRn incorporates the positively charged histidine residue. We therefore sought to incorporate an acceptable His substitution which would remain positively charged at pH 7.4 which is typical of physiological conditions (Table 12).

As an example, the thiazolyl-alanine derivative peptide **118** was weaker than the comparable His derivative SYN1327. However, methylation of the nitrogen in the thiazolidine ring introduced a positive charge at neutral pH (peptide **119**) and provided enhanced binding at pH 7.4 as compared to SYN1327.

The triazole derivative of the histidine imidazole side-chain, peptide **120**, was synthesized via reaction of a propargyl glycine-containing peptide with sodium azide under 'click chemistry' conditions.¹⁷ This analog also possesses a positive charge at neutral pH with the addition of a nitrogen to the 5-membered imidazole ring. Again, the consensus peptide motif exhibited tremendous specificity and the introduction of this change resulted in a 10-fold weaker interaction at pH 6 but only a 2-fold weaker interaction at pH 7.4, demonstrating the significance of adding a moiety capable of retaining its positive charge at neutral pH.

Over the course of studying these analogs, a trend emerged for optimal binding in the His position that ultimately captures the essential features of histidine: aromaticity and a positive charge. For example, some accepted substitutions were the pyridyl derivatives (e.g., peptide **123**) or the arginine substitution (peptide **128**); each with only a moderate loss in activity. These two favorable moieties were combined into a single molecule using 4-guanidino-Phe (peptide **129**). Peptide **129** was less active at pH 6 than the comparable His analog SYN1327; however, peptide **129** was more active at pH 7.4 due to its positive charge at neutral pH.

2.13. Peptidomimetic analogs at Gly9-Gly10-Leu11

The presence of Gly-Gly in the enclosed disulfide loop suggested a possible role for this dipeptide in allowing a unique conformation, possibly a β-turn. In addition, the lack of side-chains in this region of the peptide, and the preference of D-alanine over L-alanine (Tables 7 and 8) suggested that this region of the sequence may be amenable to further chemical manipulation. As a first attempt at removing a peptide bond, phenyl acetic acid and benzoic acid analogs were incorporated into the peptide in place of the Gly9-Gly10 dipeptide (peptides **136–139**). The meta-substituted phenyl rings resulted in weak but active peptides. In the case of peptide **139**, incorporation of 3-aminophenyl acetic acid was only 7-fold weaker than the comparable peptide **33** derivative and demonstrated that indeed the incorporation of all amide bonds is not an absolute requirement for peptide activity (Table 13).

In an attempt to restrict the conformational freedom of the Gly9-Gly10 dipeptide, various rigidified dipeptides were incorporated into the peptide (Table 13). The first of these analogs were 5-, 6-, and 7-membered lactams¹⁸ whereby the Gly10 amino group is linked to the α-carbon of Gly9 with methylene groups (peptides **140–142**). Interestingly, the favored stereocenter at Gly9 in these derivatives is the (R) configuration (peptide **141a** vs peptide **141b**). This is consistent with earlier findings that D-alanine is favored in this position over L-alanine (Tables 7 and 8). All of these lactam analogs retained significant activity and the seven-membered lactam peptide **142** was more potent than the comparable Gly9-Gly10 analog peptide **33**. Combining these analogs with the favorable N-methyl leucine substitution (peptides **145** and **146**) resulted in peptides with only slightly weaker in vitro activities as compared to SYN1327 which included the Sar-NMeLeu combination in place of Gly10-Leu11.

Table 10
Analogues of at Phe9

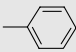
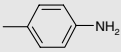
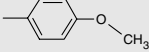
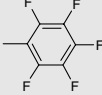
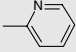
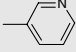
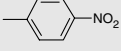
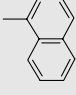
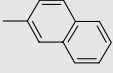
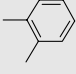
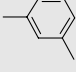
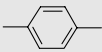
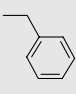
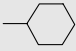
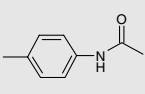
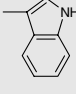
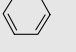
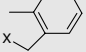
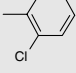
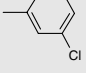
Peptide No.	Sequence	Phe analog side-chain	IC ₅₀ (μM)	K _d (pH 6) (μM)
27	QRF-Pen-TGH- <u>F</u> -GGLYPCNGP		2	0.25
85	QRF-Pen-TGH-(<u>4-amino-Phe</u>)-GGLYPCNGP		13	1
86	QRF-Pen-TGH-(<u>4-methoxy-Phe</u>)-GGLYPCNGP		100	18
87	QRF-Pen-TGH-(<u>pentafluoro-Phe</u>)-GGLYPCNGP		120	70
88	QRF-Pen-TGH-(<u>2-pyridylalanine</u>)-GGLYPCNGP		90	1.2
89	QRF-Pen-TGH-(<u>3-PyridylAla</u>)-GGLYPCNGP		60	19
90	QRF-Pen-TGH-(<u>4-nitro-Phe</u>)-GGLYPCNGP		>125	84
91	QRF-Pen-TGH-(<u>1-naphthylalanine</u>)-GGLYPCNGP		13	2.2
92	QRF-Pen-TGH-(<u>2-naphthylalanine</u>)-GGLYPCNGP		90	11
93	QRF-Pen-TGH-(<u>2-MePhe</u>)-GGLYPCNGP		1	0.20
94	QRF-Pen-TGH-(<u>3-MePhe</u>)-GGLYPCNGP		4.1	0.67
95	QRF-Pen-TGH-(<u>4-MePhe</u>)-GGLYPCNGP		1.7	0.20
96	QRF-Pen-TGH-(<u>homoPhe</u>)-GGLYPCNGP		80	7.8
97	QRF-Pen-TGH-(<u>Cha</u>)-GGLYPCNGP		31	4.5
98	QRF-Pen-TGH-(<u>PheNHAc</u>)-GGLYPCNGP		>125	270
99	QRF-Pen-TGH- <u>W</u> -GGLYPCNGP		26	2.7
100	QRF-Pen-TGH-(<u>phenylGly</u>)-GGLYPCNGP		>125	>250
101	QRF-Pen-TGH-(<u>Tic</u>)-GGLYPCNGP	 X = backbone nitrogen of amino ac	>125	>250
102	RF-Pen-TGH-(<u>2-Cl-Phe</u>)-GGLYPC		4	
103	RF-Pen-TGH-(<u>3-Cl-Phe</u>)-GGLYPC		3.7	

Table 10 (continued)

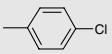
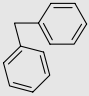
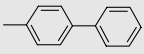
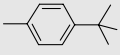
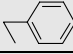
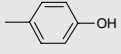
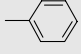
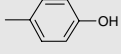
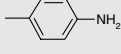
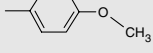
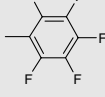
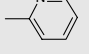
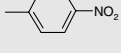
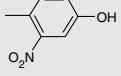

Peptide No.	Sequence	Phe analog side-chain	IC ₅₀ (μM)	K _d (pH 6) (μM)
104	RF-Pen-TGH-(<u>4-Cl-Phe</u>)-GGLYPC		43	
105	RF-Pen-TGH-(<u>3,3-Di-Phe</u>)-GGLYPC		32	
106	RF-Pen-TGH-(4,4-Bi-Phe)-GGLYPC		>125	
107	RF-Pen-TGH-(<u>4-tert-Butyl-Phe</u>)-GGLYPC		>125	
108	RF-Pen-TGH-((D/L)- <u>betamethylPhe</u>)-G-Sar-NMeLeu-YPC		16	

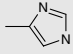
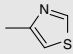
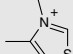
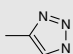
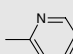
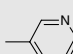
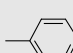
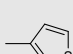
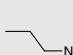
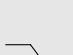
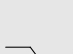
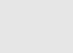
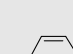
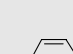
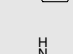
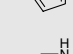
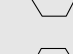
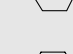
Table 11Analogues of SYN746 and peptide **27** at Tyr12

Peptide No.	Sequence	Tyr analog chain	(IC ₅₀ μM)	K _d (pH 6) (μM)
SYN746	QRFCTGHFGGL- <u>Y</u> -PCNGP		40 ± 15 (n = 4)	5.1
109	QRFCTGHFGGL-F-PCNGP		>125	230
27	QRF-Pen-TGHFGGL-<u>Y</u>-PCNGP		2	0.25
110	QRF-Pen-TGHFGGL-(<u>4-amino-Phe</u>)-PCNGP		110	34
111	QRF-Pen-TGHFGGL-(4-methoxyPhe)-PCNGP		120	31
112	QRF-Pen-TGHFGGL-(<u>pentafluoroPhe</u>)-PCNGP		>125	72
113	QRF-Pen-TGHFGGL-(<u>2-pyridylAla</u>)-PCNGP		>125	120
114	QRF-Pen-TGHFGGL-(<u>3-pyridylAla</u>)-PCNGP		92	34
115	QRF-Pen-TGHFGGL-(<u>4-nitro-Phe</u>)-PCNGP		122	180
116	QRF-Pen-TGHFGGL-(<u>2-nitro-Tyr</u>)-PCNGP		>125	290
117	QRF-Pen-TGHFGGL-(<u>4-fluoro-Phe</u>)-PCNGP		26	2.2

Bicyclic 5,5- and 6,5-thiazolidine lactam peptidomimetics are known in the literature to mimic β -turn structures.¹⁹ When both of the constituent amino acids in the dipeptide mimic are in the *D* configuration, the 5,5- and 6,5-dipeptides were found to mimic a type II β -turn.³⁰ When the constituent amino acids of the 6,5-dipeptide are both in the *L* configuration, the dipeptide mimic was found to mimic a type II' β -turn.²⁰ These bicyclic analogs were synthesized as their Fmoc-protected precursors and incorporated into the peptide synthesis protocol (Table 13). Since our previous work demonstrated that the *D* stereochemistry is favored for both glycine amino acids in the putative β -turn, both 5,5- and 6,5-bicyclic analogs were syn-

thesized with *D,D* stereocenters. The incorporation of the 5,5-bicyclic dipeptides into the peptide sequence (peptides **143a** and **143b**) resulted in two separable compounds, likely diastereomers at the bridgehead carbon as a result of the bicyclic cyclization as observed previously by Subasinghe et al.³⁰ and Baldwin et al.²¹ When these 5,5-bicyclic dipeptides were incorporated into the peptide sequence, both diastereomers were >5-fold weaker than the comparable Gly9-Gly10 analog. In contrast, the 6,5-bicyclic analog peptide **144** was nearly equipotent with the Gly-Gly analog which suggests that the Gly-Gly dipeptide may form a type II β -turn. Further structural information will be required to confirm this hypothesis.

Table 12
Peptide analogs of SYN1327 at His7

Peptide No.	Sequence	His analog side chain	IC ₅₀ (μM)	K _d (pH 6) 1 μM	K _d (pH 7.4) (μM)
SYN1327	RF-Pen-TG- <u>His</u> -FG-Sar-NMeLeu-YPC		0.57 ± 0.20 (n = 11)	0.031 ± 0.004 (n = 3)	0.17 ± 0.020 (n = 3)
118	RF-Pen-TG- <u>Thz</u> -FG-Sar-NMeLeu-YPC		1.6	0.84	1.1
119	RF-Pen-TG- <u>Thz(Me)</u> -FG-Sar-NMeLeu-YPC-CONH2		2.4	0.11	0.11
120	RF-Pen-TG- <u>triazolylAla</u> -FG-Sar-NMeLeu-YPC		5.7	0.32	0.36
121	RF-Pen-TG-2 <u>PyridylAla</u> -FG-Sar-NMeLeu-YPC		6.2	.33	0.41
122	RF-Pen-TG-3 <u>PyridylAla</u> -FG-Sar-NMeLeu-YPC		1.2	.064	0.26
123	RF-Pen-TG-(4- <u>PyridylAla</u>)-FG-Sar-NMeLeu-YPC		1.3	0.067	0.28
124	RF-Pen-TG- <u>ThienylAla</u> -FG-Sar-NMeLeu-YPC		45	2	3
125	RF-Pen-TG- <u>Dab</u> -FG-Sar-NMeLeu-YPC		16	1.2	1.2
126	RF-Pen-TG- <u>Orn</u> -FG-Sar-NMeLeu-YPC		12	1.3	1.2
127	RF-Pen-TG- <u>Lys</u> -FG-Sar-NMeLeu-YPC		40	1.3	1.1
128	RF-Pen-TG- <u>Arg</u> -FG-Sar-NMeLeu-YPC		5.5	0.5	0.5
129	RF-Pen-TG-4 <u>GuanylPhe</u> -FG-Sar-NMeLeu-YPC		1.7	0.074	0.073
130	RF-Pen-TG-4 <u>aminoPhe</u> -FG-Sar-NMeLeu-YPC		4.6	0.22	1.1
131	RF-Pen-TG-(2- <u>PyrrolidinylAla</u>)-FG-Sar-NMeLeu-YPC		150	8.4	13
132	RF-Pen-TG-(3- <u>PiperidylAla</u>)-FG-Sar-NMeLeu-YPC		6.3	0.66	0.86
133	RF-Pen-TG-(4- <u>PiperidylAla</u>)-FG-Sar-NMeLeu-YPC		85	5.2	6.4
134	RF-Pen-TG <u>EFG</u> -Sar-NMeLeu-YPC		27	3.3	4.2
135	RF-Pen-TG <u>Δ</u> FG-Sar-NMeLeu-YPC	CH ₃	>100	9.9	13

Backbone lactam incorporation was also briefly studied in the context of the Gly10-Leu11 dipeptide (Table 14). As was the case with the Gly9-Gly10 derivatives, the stereocenter favored a (*R*) configuration but still provided peptides with weaker activity than that of Gly9-Gly10.

2.14. Disulfide replacement with lactam bridges

The replacement of the disulfide bond with a lactam bridge may enhance the peptide's *in vivo* stability by removing the chemically reversible disulfide linkage. This approach was studied thoroughly

Table 13Peptidomimetic analogs of peptide **33** and SYN1327 at Gly9-Gly10

Peptide No.	Sequence	X Description	X Structure	IC ₅₀ (μM)	K _d (pH 6) (μM)
33	RF-Pen-TGHF-X-LYPC	Gly-Gly		2.0	0.17
136	RF-Pen-TGHF-X-LYPC	4-aminomethyl-benzoic acid		>125	nd
137	RF-Pen-TGHF-X-LYPC	(3-aminomethyl)-benzoic acid		57	nd
138	RF-Pen-TGHF-X-LYPC	4-aminophenyl acetic acid		>125	nd
139	RF-Pen-TGHF-X-LYPC	3-aminophenyl acetic acid		14	nd
140	RF-Pen-TGHF-X-LYPC	3(R)-3-amino-2-oxo-1-pyrrolidine-acetic acid		2.3	0.28
141a	RF-Pen-TGHF-X-LYPC	3(R)-amino-2-oxo-1-piperidine-acetic acid		0.66	0.16
141b	RF-Pen-TGHF-X-LYPC	3(S)-amino-2-oxo-1-piperidine-acetic acid		7.2	0.67
142	RF-Pen-TGHF-X-LYPC	3(R)-3-amino-2-oxo-1-azepine-acetic acid		0.64	0.103
143a	RF-Pen-TGHF-X-LYPC	5,5-bicyclic dipeptide mimic		13	0.99
143b	RF-Pen-TGHF-X-LYPC	5,5-bicyclic dipeptide mimic		23	nd
144	RF-Pen-TGHF-X-LYPC	6,5-bicyclic dipeptide mimic		2.2	0.32
SYN1327	RF-Pen-TGHF-X-NMeLeu-YPC	Gly-Sar		0.57 ± 0.20 (n = 11)	0.031 ± 0.004 (n = 3)
145	RF-Pen-TGHF-X-NMeLeu-YPC	(3R)-3-amino-1-carboxymethyl-valerolactam		0.53	0.043
146	RF-Pen-TGHF-X-NMeLeu-YPC	3(R)-3-amino-2-oxo-1-azepine acetic acid		0.62	0.044

using natural and unnatural amino acids with complementary carboxy and amino side-chains (Table 15). Although no clear trend emerged from the study, a preference for Asp in the first cysteine position was evident. Interestingly, the combination of Asp-Lys (peptide **152**) is approximately 3-fold more potent than the unoptimized phage sequence SYN746 which incorporates a cysteine-cysteine disulfide. However, the combination of the Pen-Cys disulfide is clearly preferred over all other forms of peptide cyclization studied. Interestingly, nearly all of the peptides remain active in some form, albeit more weakly. This is consistent with the

data from the disulfide analogs (Table 4) which demonstrated that longer disulfide-linked loops do not affect the peptide activity.

2.15. Linear analogs

The great flexibility in the mode of cyclization and the success in optimizing the Gly9-Gly10 motif led to the study of non-cyclized analogs of SYN746 (Table 16). Utilization of optimized moieties in place of the Gly9-Gly10 motif in conjunction with valine for penicillamine, it was possible to generate linear peptides (peptides

Table 14
Peptidomimetic analogs of peptide **27** at Gly10-Leu11

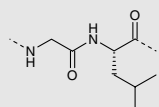
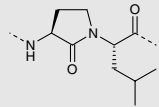
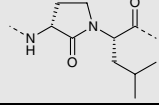
Peptide No.	Sequence	X Description	X Structure	IC ₅₀ (μM)
27	QRF-Pen-TGHFG-X-YPNCNP	Gly-Leu		2.0
147	RF-Pen-TGHFG-X-YPNC	L,L-Friedinger's lactam		19
148	QRF-Pen-TGHFG-X-YPNCNP	D,L-Friedinger's lactam		4.9

Table 15
Lactam-cyclized peptide analogs of SYN746

Peptide No.	Sequence ^a	Bridge Length ^b	IC ₅₀ (μM)	K _d (pH 6) (μM)
SYN746	QRF-C-TGHFGGLYP-C-NGP	4	40 ± 15 (n = 4)	5.1
27	QRF-Pen-TGHFGGLYP-C-NGP	4	2	0.25
149	QRF- <u>Asp</u> -TGHFGGLYP- <u>Dap</u> -NGP	4	32	4.5
150	QRF- <u>Asp</u> -TGHFGGLYP- <u>Dab</u> -NGP	5	68	17
151	QRF- <u>Asp</u> -TGHFGGLYP- <u>Orn</u> -NGP	6	16	2.7
152	QRF- <u>Asp</u> -TGHFGGLYP- <u>Lys</u> -NGP	7	10	1.2
153	QRF- <u>Glu</u> -TGHFGGLYP- <u>Dap</u> -NGP	5	71	9.6
154	QRF- <u>Glu</u> -TGHFGGLYP- <u>Dab</u> -NGP	6	86	22
155	QRF- <u>Glu</u> -TGHFGGLYP- <u>Orn</u> -NGP	7	80	15
156	QRF- <u>Glu</u> -TGHFGGLYP- <u>Lys</u> -NGP	8	100	27
157	QRF- <u>Dap</u> -TGHFGGLYP- <u>Asp</u> -NGP	4	120	nd
158	QRF- <u>Dab</u> -TGHFGGLYP- <u>Asp</u> -NGP	5	31	8.4
159	QRF- <u>Orn</u> -TGHFGGLYP- <u>Asp</u> -NGP	6	120	nd
160	QRF- <u>Lys</u> -TGHFGGLYP- <u>Asp</u> -NGP	7	60	10
161	QRF- <u>Dap</u> -TGHFGGLYP- <u>Glu</u> -NGP	5	>125	nd
162	QRF- <u>Dab</u> -TGHFGGLYP- <u>Glu</u> -NGP	6	81	4.8
163	QRF- <u>Orn</u> -TGHFGGLYP- <u>Glu</u> -NGP	7	30	nd
164	QRF- <u>Lys</u> -TGHFGGLYP- <u>Glu</u> -NGP	8	33	1.2

^a There is an amide bond between the side-chains of the underlined amino acids; Dab, 1,3-diaminobutyric acid; Dap, 1,2-diaminopropionic acid; Orn, ornithine.

^b 'Bridge length' refers to the number of atoms in the lactam/disulfide bridge.

166–168) roughly equipotent to the unoptimized cyclic phage peptide SYN746.

2.16. In vitro peptide stability to subtilisin

It was hypothesized that some non-natural substitutions may provide enhanced protease stability. Therefore, concurrent with studying the in vitro activity of analogs of SYN722, the in vitro stability of various analogs to protease digestion was also investigated using LC/MS and LC/MS–MS for detection of intact peptide and to study sites of cleavage.²² Peptides **27**, **74**, and **169** were representative peptide analogs with stabilizing *N*-methyl or *D*-amino acids (Table 17, Fig. 2). Subtilisin is a serine endoprotease and was selected for these model studies due to its specificity for a broad range of peptide bonds.²³

It was found that the core peptide sequence of peptide **27** possessed three peptide bonds that were prone to cleavage by subtilisin: Gly6-His7, Phe8-Gly9 and Leu11-Tyr12 (Fig. 2). Additionally, the *N*- and *C*-terminal residues were also prone to digestion. Incorporation of *D*-Ala and *N*-MeLeu in peptide **74** effectively stabilized both the Phe8-Gly9 bond and Leu11-Tyr12 under the experimental conditions, but the peptide was still prone to cleavage at Gly6-His7. Peptide **169** possessed an additional stabilizing substitution

Table 16
Linear Peptides Analogs of SYN746 at Gly9-Gly10

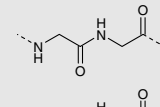
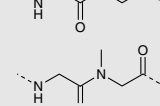
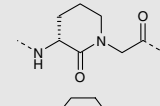
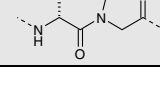

Peptide No.	Sequence	X Description	X Structure	IC ₅₀ (μM)	K _d (pH 6) (μM)
SYN746	QRF-TGHF-X-LYPNCNP	Gly-Gly		40 ± 15 (n = 4)	5.1
165	QRF- <u>S</u> -TGHF-X-LYP- <u>S</u> -NGP	Gly-Gly		>125	230
166	RF-V-TGHF-X-NMeLeu-YPA	Gly-Sar		37	1.85
167	RF-V-TGHF-X-LYPA	3(R)-amino-2-oxo-1-piperidine-acetic acid		38	3.3
168	RF-V-TGHF-X-LYPA	3(R)-3-amino-2-oxo-1-azepine acetic acid		23	2.3

Table 17
Effect of subtilisin on peptide stability

Peptide No.	Sequence	IC ₅₀ (μM)	% Intact ^a after 1 h subtilisin	% Intact ^a after 18 h subtilisin
27	QRF-Pen-TGHFGGLYPC-NGP	2	5	0
74	QRF-Pen-TGHF-a-G-NMeLeu-YPC-NGP	3.2	5	0
169	RF-Pen-NMeAla-GHFaG-NMeLeu-YPC	8	100	95

^a % Intact does not include amino acids non-essential to peptide activity including the N-terminal Gln residue or the C-terminal Asn-Gly-Pro residues.

by incorporating *N*-MeAla for Thr. This prevented the cleavage at the Gly6-His7 bond. Peptide **169** also incorporated N- and C-terminal truncations which prevented additional digestion. Peptide **169** was therefore the most stable of the three peptides that were tested in vitro. Peptide **169** was ~95% intact after 18 h under the assay conditions while both peptides **33** and **74** were only 5% intact after 1 h (Table 17). However, the substitution of *N*-MeAla for Thr in peptide **169** reduced the in vitro activity approximately 4-fold, therefore depending on the in vivo relevance of this in vitro stability model, this substitution may not be preferred.

3. Discussion

We previously demonstrated that peptide dimer SYN1436 can bind with high affinity to shFcRn, block the binding of hIgG to hFcRn, and inhibit the natural recycling mechanism of circulating IgG in cynomolgus monkeys thereby reducing IgG concentrations in vivo.¹² The core sequence of each monomeric peptide in the SYN1436 dimer was derived from the phage display hit SYN722.

The consensus peptide motif, **GHFGGXY** where **X** is preferred as a hydrophobic amino acid, was discovered in the context of three different disulfide placements around the motif, each enclosing 11 amino acids and each peptide possessing nearly equipotent activity in vitro. This change in register of the motif within the cysteine disulfide loop is very interesting considering the specificity of the peptide–protein interaction and suggests that the method of cyclization is not as critical as the core residues themselves. This was evident over the course of studying the analogs of SYN722 since the disulfide loop could be modified with longer disulfides (homocysteine disulfides) or with various lactams with minimal loss in activity, and sometimes, with an improvement in activity. Furthermore, the fact that certain linear peptide analogs possessing optimized residues were found to be as active as the original phage hit SYN722 suggests that only a very small number of interactions are responsible for the majority of the peptide–FcRn binding energy. These specific interactions likely include Gly6, His7,

Phe8 and Tyr12, although Gly6 may only be required in the context of this peptide structure. This is particularly interesting since it is known that IgG, the natural ligand for human FcRn, contains three histidine residues and one tyrosine residue (His310, His433, His435, and Tyr436) at the binding interface.^{24,25} The consensus peptide motif may be mimicking these Fc:FcRn binding interactions, despite having no homology to Fc. Further structural information will be needed to better understand the peptide:FcRn interaction.

The substitution that resulted in the largest enhancement in affinity for FcRn was the incorporation of L-penicillamine for Cys4. Although the nature of this enhancement is not presently understood, the extra β-dimethyl groups of penicillamine may rigidify the peptide disulfide and better preorganize the overall peptide structure for receptor binding. Additionally, the two extra methyl groups may be involved in a binding interaction directly with FcRn. Interestingly, the peptide phage hit SYN723 also incorporates a β-dimethyl group in the equivalent position via its valine residue.

IgG binds to FcRn using histidine residues resulting in pH-dependent binding to FcRn: binding at pH 6 and minimal binding at pH 7.4. For an optimized FcRn antagonist, it is likely that binding at both pH 6 and pH 7.4 would be favored such that the peptide could remain bound to its target for as long as possible. Accordingly, peptide analogs containing various histidine derivatives were synthesized. None of the analogs demonstrated improved binding at pH 6 over that of SYN1327, which contains a histidine. However, peptide **129** containing the *p*-guanylylphenylalanine substitution was more potent at pH 7.4 and further studies will be performed to determine if the higher affinity at pH 7.4 is an advantage in vivo.

Peptide phage display is a powerful tool to discover novel peptide ligands for protein–protein interactions by screening pools of billions of peptides.²⁶ One limitation to the technique, however, is the inherent limitation to the 20 naturally occurring amino acids. Although other biological display techniques are beginning to incorporate unnatural components to their screens,²⁷ these screens still largely rely on naturally occurring amino acids and linkages. In this work, peptide phage display was coupled with extensive chemical optimization to generate peptide ligands with a 50- to 100-fold increase in activity by the incorporation of non-natural amino acids; an increase which may not have been discovered using biological techniques alone.

4. Conclusions

The structure–activity relationships of peptide SYN722 led to the optimization of the peptide:hFcRn interaction and greater inhibition of the IgG:FcRn interaction. The peptide lead, SYN722, was

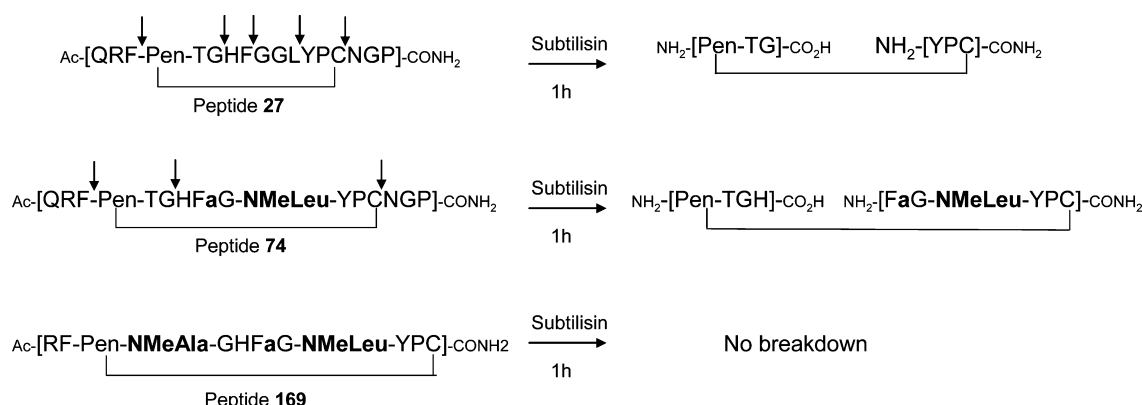


Figure 2. Schematic representation of the observed cleavage sites within peptides **27**, **74** and **169** after treatment with subtilisin for 1 hour.

truncated from 25 to 13 amino acids, followed by the addition of four methyl groups to generate peptide SYN1327. SYN1327 possessed ~50- to 100-fold greater affinity for shFcRn than its parent peptide with an equivalent enhancement in its inhibition of the IgG:FcRn interaction as determined by in vitro assays. SYN1327 is the constituent monomeric peptide found in peptide dimer SYN1436 which was able to significantly reduce circulating IgG levels in cynomolgus monkeys. Further structural studies on the peptides should enable the development of peptidomimetics and/or small molecule FcRn antagonists.

5. Experimental

5.1. Peptide synthesis

Peptide synthesis was performed using solid-phase methods either manually with a fritted round bottom flask or by using an Advanced Chemtech 396-Omega synthesizer (Advanced Chemtech, Louisville, KY). Standard Fmoc/tBu protocols were used²⁸ in combination with a Rink amide resin (Novabiochem, San Diego, CA) or PAL-PEG-PS (Applied Biosystems, Foster City, CA) to yield C-terminal amides upon cleavage. The coupling reagents were 2-(1H-Benzotriazole-1-yl)-1,1,3,3-tetramethyluronium hexafluorophosphate (HBTU) and N-hydroxybenzotriazole (HOBt) (Novabiochem, San Diego, CA). The base was diisopropylethylamine (DIEA) (Sigma-Aldrich, St. Louis, MO), and *N,N*-dimethylformamide (DMF) was the solvent (EM Science, Kansas City, MO). The typical synthesis cycle involved 2× 10 min deprotection steps with 20% piperidine in DMF, 2× 30 min amino acid couplings with HOBt/HBTU and a 10-min capping step with acetic anhydride/HOBt. All amino acids were obtained from commercial sources (Novabiochem, Anaspec, Bachem, Chem-Impex) unless otherwise noted below. Peptides were cleaved from the resin by treatment for 2 h with either 95% trifluoroacetic acid (TFA); 2.5% ethanedithiol; 1.5% triisopropylsilane and 1% water or 95% TFA and 5% triisopropyl silane. The crude peptides in the cleavage mixture were precipitated with ice-cold ether, centrifuged and triturated three more times with ether. All peptides are acetylated at the N-terminus and amidated at the C-terminus unless otherwise noted. Crude cysteine-containing peptides were oxidized to their corresponding disulfides by dissolving the peptides to a concentration of 1 mg/ml in a 4:1 mixture of acetic acid and water. Ten molar equivalents of iodine (1 M solution in water, Sigma-Aldrich, St. Louis, MO) were added to the solution and the reaction mixture was mixed for one hour at room temperature. The reaction was stopped by the progressive addition of 1 M sodium thiosulfate (Sigma-Aldrich, St. Louis, MO) until a clear solution was obtained. The reaction mixture was concentrated in vacuo and purified using a reversed phase HPLC system equipped with a 250 mm × 21.2 mm C18 column (Phenomenex, Torrance, CA) using a flow rate of 20 mL/min. The eluent chosen for the HPLC purification step was a gradient of acetonitrile in water containing 0.1% TFA. Appropriate fractions were collected, pooled and lyophilized. All peptides were ≥90% pure as determined by reversed phase analytical HPLC using a 250 mm × 2 mm C18 column (Phenomenex, Torrance, CA) and gradients of acetonitrile (+0.02% TFA and 0.08% formic acid) in water (+0.02% TFA and 0.08% formic acid). Peptide identities were confirmed using electrospray mass spectrometry (Mariner ES-MS, Applied Biosystems, Foster City, CA); all peptides reported herein resulted in their expected *m/z* values. See [supporting information](#) for all calculated and observed MS data. Peptides **141a**, **141b**, **145**, and **167**, containing 3-amino-2-oxo-1-piperidine-acetic, were prepared by first synthesizing the *N*-Fmoc derivative of 3(*R,S*)-3-amino-2-oxo-1-piperidine-acetic acid as described in the literature.²⁹ This building block was then incorporated into each peptide according to standard protocols.

Peptide **140**, containing 3(*R*)-3-amino-2-oxo-1-pyrrolidine acetic acid, was prepared by first synthesizing *N*-Fmoc derivative of 3(*R*)-3-amino-2-oxo-1-pyrrolidine acetic acid described in the literature.²⁹ This building block was then incorporated into peptide **140** using standard protocols. Peptides **143a** and **143b**, containing the 5,5-bicyclic dipeptide mimic, were prepared by incorporating the *N*-Fmoc derivative of the 5,5-bicyclic dipeptide mimic that was synthesized as described in the literature,³⁰ with the exception that all D-amino acids were used as starting materials. Peptide **144**, containing the 6,5-bicyclic dipeptide mimic, was prepared by incorporating the *N*-Fmoc derivative of the 6,5-bicyclic dipeptide mimic that was synthesized as described in the literature,³¹ with the exception that all D-amino acids were used as starting materials. Peptide **147**, containing the (L,L)-Freidinger's lactam, was prepared by incorporating the Fmoc derivative of the (L,L)-Freidinger's lactam that was synthesized as described in the literature¹⁸ with the exception that L-methionine was used instead of D-methionine.

5.1.1. Peptide 119

The resin containing the fully protected peptide *Ac-Arg(Pbf)-Phe-Pen(Trt)-Thr(tBu)-Gly-Thiazolylalanine-Phe-Gly-Sar-NMeLeu-Tyr(tBu)-Pro-Cys(Trt)-resin* was suspended in dichloromethane under nitrogen. Ten molar equivalents of 2,4,6-tri-*tert*-butylpyridine (Sigma-Aldrich, St. Louis, MO) were added to the suspension followed by five molar equivalents of methyl-trifluoromethanesulfonate (Sigma-Aldrich, St. Louis, MO). The reaction was mixed for 4 h, rinsed with dichloromethane (DCM), DMF and finally with DCM again. The peptide was cleaved from the resin, oxidized and purified by HPLC as described above to yield the *N*-methyl-thiazolium peptide **119**. MS (ESI, pos mode, H₂O/CH₃CN + 0.02% formic acid/0.08% TFA) for C₇₃H₁₀₃N₁₈O₁₆S₃: [M+H]²⁺ calcd 793.0; found 792.4.

5.1.2. Peptide 120

The peptide resin: *Ac-Arg(Pbf)-Phe-Pen(Trt)-Thr(tBu)-Gly-PropargylGly-Phe-Gly-Sar-NMeLeu-Tyr(tBu)-Pro-Cys(Trt)-CONH₂* was treated with 30 equiv of copper sulfate, 30 equiv of ascorbic acid and 10 equiv of sodium azide in a solution of 100 mM sodium phosphate buffer at pH 7.5 with 33% ethanol, 10% acetonitrile, 10% DMF. The reaction proceeded for 2 h and the mixture was purified by HPLC as described above to yield the 1,2,3-triazole side-chain-containing peptide **120**. MS (ESI, pos mode, H₂O/CH₃CN + 0.02% formic acid/0.08% TFA) for C₇₁H₁₀₀N₂₀O₁₆S₂: [M+H]²⁺ calcd 777.9; found 777.3.

5.1.3. Peptide 142

(*R*)-3-(Boc-amino)-2-oxo-1-azepine (Chem-Impex, 250 mg, 0.87 mmol) was treated with DCM/TFA (4:1, 20 mL) and 300 μL of water. After 1h, the reaction mixture was evaporated in vacuo, precipitated with ice-cold ether, and evaporated in vacuo. To this free amino acid (0.87 mmol) in DMF/water (1:1, 20 mL) was added Fmoc-OSu (Novabiochem, 0.87 mmol) and NaHCO₃ (5 equiv, 4.35 mmol, 365 mg) and stirred for 1 h. The reaction mixture was poured onto 5% citric acid, extracted three times with ethyl acetate. The organic extracts were then washed three times with 5% citric acid, brine, dried over MgSO₄ and evaporated in vacuo to afford a white solid. MS (ESI, pos mode, H₂O/CH₃CN + 0.02% formic acid/0.08% TFA) for C₂₃H₂₄N₂O₅: [M+H]⁺ calcd 409.5; found 409.3. This building block was subsequently incorporated into the peptide synthesis protocols to afford peptide **142**.

5.2. Synthesis of peptides cyclized using lactam bridges

Lactam-cyclized peptides were synthesized by solid-phase synthesis as outlined above with the exception that the following ami-

no acids were used as substitutes for the two cysteines: Fmoc-Lys(Aloc)-OH, Fmoc-Orn(Aloc)-OH, Fmoc-Dab(Aloc)-OH and Fmoc-Dap(Aloc)-OH, Fmoc-Glu(OAllyl)-OH and Fmoc-Asp(OAllyl)-OH (Bachem, Torrance, CA). Following the synthesis of the fully protected peptides on resin, the resin was swollen in dichloromethane, purged with nitrogen and treated with 0.1 molar equivalents of tetrakis-(triphenylphosphine)palladium(0) (Sigma–Aldrich, St. Louis, MO) and 30 mequiv of phenylsilane (Sigma–Aldrich, St. Louis, MO) and the reaction was allowed to proceed for 3 h. The resin was washed with DCM, DMF and finally five additional times with a solution of 1% (v/v) triethylamine and 1% (w/v) diethyldithiocarbamic acid in DMF. An additional washing step with DMF was followed by treatment of the resin with benzotriazole-1-yl-oxy-tris-pyrrolidino-phosphonium hexafluorophosphate (PyBOP) (Novabiochem, San Diego CA) and DIEA for 16 h. The peptides were cleaved from the resin and purified as described above.

5.3. Surface plasmon resonance

Peptide affinity constants for shFcRn were determined using a Biacore 3000 instrument with soluble human FcRn (shFcRn) conjugated to the dextran surface of a CM5 sensor chip as described previously.¹² The equilibrium response observed for each peptide dilution was plotted against concentration and analyzed using the steady state affinity model (included in the BiaEval software) to determine K_d values.

5.4. IgG Competition ELISA assay

Peptide derivatives were assayed for binding to shFcRn in competition with hIgG as described previously.¹² Briefly, biotinylated shFcRn immobilized on a neutravidin plate was incubated with 3 nM hIgG and peptide competitor for 2 h at 37 °C. The plate was washed with buffer and residual hIgG in the well was quantified using peroxidase-conjugated hIgG specific Fab fragments. The concentration of peptide capable of inhibiting 50% of the IgG binding to shFcRn was designated the IC_{50} .

5.5. In vitro stability studies with subtilisin

Peptides (**27** and **74** and **169**) were dissolved in PBS at a concentration of 0.3 mg/mL and treated with a 470-fold molar excess of Subtilisin Carlsberg (Calbiochem) such that the final reaction volume was 100 μ L. The reaction was incubated at room temperature, and at each timepoint, 25 μ L of the enzymatic reaction was removed and quenched with the addition of 5 μ L of 1 M sodium acetate pH 4.7 and 50 μ L of acetonitrile. The samples were evaporated in vacuo, reconstituted in 50 μ L of acidified water (water + 0.08% formic acid and 0.02% TFA), centrifuged through a 10-kDa filter membrane (Nanosep 10K Omega, Pall Corp), and injected onto a LC/MS/MS (Thermo LCQ) equipped with a C18 reversed phase column for analysis using gradients of acetonitrile (0.08% formic acid

and 0.02% TFA) in water (0.08% formic acid and 0.02% TFA) as the eluent. See [Supporting information](#) file for LC/MS/MS data.

Supplementary data

Supplementary data associated with this article can be found, in the online version, at [doi:10.1016/j.bmc.2008.05.004](https://doi.org/10.1016/j.bmc.2008.05.004).

References and notes

- Ghetie, V.; Ward, E. S. *Annu. Rev. Immunol.* **2000**, *18*, 739–766.
- Roopenian, D. C.; Akilesh, S. *Nat. Rev. Immunol.* **2007**, *7*, 715–725.
- Roopenian, D. C.; Christianson, G. J.; Sproule, T. J.; Brown, A. C.; Akilesh, S.; Jung, N.; Petkova, S.; Avanesian, L.; Choi, E. Y.; Shaffer, D. J.; Eden, P. A.; Anderson, C. L. *J. Immunol.* **2003**, *170*, 3528–3533.
- Borvak, J.; Richardson, J.; Medesan, C.; Antohe, F.; Radu, C.; Simionescu, M.; Ghetie, V.; Ward, E. S. *Int. Immunol.* **1998**, *10*, 1289–1298.
- Akilesh, S.; Christianson, G. J.; Roopenian, D. C.; Shaw, A. S. *J. Immunol.* **2007**, *179*, 4580–4588.
- Ober, R. J.; Martinez, C.; Vaccaro, C.; Zhou, J.; Ward, E. S. *J. Immunol.* **2004**, *172*, 2021–2029.
- Ober, R. J.; Martinez, C.; Lai, X.; Zhou, J.; Ward, E. S. *Proc. Nat. Acad. Sci. U.S.A.* **2004**, *101*, 11076–11081.
- Akilesh, S.; Petkova, S.; Sproule, T. J.; Shaffer, D. J.; Christianson, G. J.; Roopenian, D. C. *J. Clin. Invest.* **2004**, *113*, 1328–1333.
- Li, N.; Zhao, M.; Hilario-Vargas, J.; Prisanh, P.; Warren, S.; Diaz, L. A.; Roopenian, D. C.; Liu, Z. *J. Clin. Invest.* **2005**, *115*, 3440–3450.
- Lui, L.; Garcia, A. M.; Santoro, H.; Zhang, Y.; McDonnell, K.; Dumont, J.; Bitonti, A. *J. Immunol.* **2007**, *178*, 5390–5398.
- Petkova, S. B.; Akilesh, S.; Sproule, T. J.; Christianson, G. J.; Khabbaz, H. A.; Brown, A. C.; Presta, L. G.; Meng, Y. G.; Roopenian, D. C. *Int. Immunol.* **2006**, *18*, 1759–1769.
- Mezo, A. R.; McDonnell, K. A.; Tan Hehir, C. A.; Low, S. C.; Palombella, V. J.; Stattel, J. M.; Kamphaus, G. D.; Fraley, C.; Zhang, Y.; Dumont, J. D.; Bitonti, A. *J. Proc. Nat. Acad. Sci. U.S.A.* **2008**, *105*, 2337–2342.
- Sagan, S.; Karoyan, P.; Lequin, O.; Chassaing, G.; Lavielle, S. *Curr. Med. Chem.* **2004**, *11*, 2799–2822.
- Favre, M.; Moehle, K.; Jiang, L.; Pfeiffer, B.; Robinson, J. A. *J. Am. Chem. Soc.* **1999**, *121*, 2679–2685.
- Stranger, H. E.; Gellman, S. H. *J. Am. Chem. Soc.* **1998**, *120*, 4236–4237.
- Sato, K.; Nagai, U. *J. Chem. Soc., Perkin Trans. 1* **1986**, 1231–1234.
- Wang, Q.; Chan, T. R.; Hilgraf, R.; Fokin, V. V.; Sharpless, K. B.; Finn, M. G. *J. Am. Chem. Soc.* **2003**, *125*, 3192–3193.
- Friedinger, R. M. *J. Med. Chem.* **2003**, *46*, 5553–5566.
- Hanessian, S.; McNaughton-Smith, G.; Lombart, H.-G.; Lubell, W. D. *Tetrahedron* **1997**, *53*, 12789–12854.
- Nagai, U.; Sato, K.; Nakamura, R.; Kato, R. *Tetrahedron* **1993**, *49*, 3577–3592.
- Baldwin, J. E.; Freeman, R. T.; Lowe, C.; Schofield, C. J.; Lee, E. A. *Tetrahedron* **1989**, *45*, 4537–4550.
- See [Supporting information](#) for LC/MS/MS data.
- Wells, J. A.; Estell, D. A. *Trends Biochem. Sci.* **1988**, *13*, 291–297.
- Martin, W. L.; West, A. P., Jr.; Gan, L.; Bjorkman, P. J. *Mol. Cell* **2001**, *7*, 867–877.
- Shields, R. L.; Namenuk, A. K.; Hong, K.; Meng, Y. G.; Rae, J.; Briggs, J.; Xie, D.; Lai, J.; Stadlen, A.; Li, B., et al. *J. Biol. Chem.* **2001**, *276*, 6591–6604.
- Ladner, R. C.; Sato, A. K.; Gorzelany, J.; de Souza, M. *Drug Discov. Today* **2004**, *9*, 525–529.
- Millward, S. W.; Fiacco, S.; Austin, R. J.; Roberts, R. W. *ACS Chem. Biol.* **2007**, *2*, 625–634.
- Fmoc Solid Phase Peptide Synthesis: A Practical Approach*; Chan, W. C., White, P. D., Eds.; Oxford University Press, Inc.: New York, 2000.
- Freidinger, R. M.; Perlow, D. S.; Veber, D. F. *J. Org. Chem.* **1982**, *47*, 104–109.
- Subasinghe, N. L.; Bontems, R. J.; McIntee, E.; Mishra, R. K.; Johnson, R. L. *J. Med. Chem.* **1993**, *36*, 2356–2361.
- Etzkorn, F. A.; Guo, T.; Lipton, M. A.; Goldberg, S. D.; Bartlett, P. A. *J. Am. Chem. Soc.* **1994**, *116*, 10412–10425.